ARCHIVES OF ELECTRICAL ENGINEERING VOL. X(Y), pp. 1-22 (2027)

This paper has been accepted for publication in the AEE journal. This is the version, which has not been fully edited and content may change prior to final publication.
Citation information: DOI 10.24425/aee.2027.8065

Adaptive generator-torque-driven energy management with state-of-charge regulation for power-split hybrid electric vehicles

PRASHANTHI PEDDIREDDIGARI[1], SRI GOWRI KOLLI[2]*

[1]*Research Scholar JNTUA, Government Polytechnic for Women, Department of EEE Kadapa-516002, A.P., India*

[2]*G.Pulla Reddy Engineering College, Department of EEE Kurnool-518007, A.P., India*
*e-mail: shivashanthi@gmail.com, *srigowri.eee@gprec.ac.in*

Early Access

Abstract: Power-split hybrid electric vehicles (PS-HEVs) have gained considerable attention owing to their potential to improve fuel efficiency through the coordinated operation of the internal combustion engine, electric motor, generator, and battery. However, the coupling introduced by the planetary gear set complicates energy management. This paper presents an adaptive energy management strategy (EMS) based on generator-torque control and battery state-of-charge (SOC) regulation. The proposed approach uses generator torque as a principal supervisory control variable alongside vehicle speed, traction power demand, and battery SOC to coordinate power distribution. The strategy is implemented in a MATLAB/Simulink-based PS-HEV model and compared with three benchmark energy management strategies. Under the UDDS drive cycle, the proposed Case 4 consumes 0.1249 kg of fuel, compared with 0.2206 kg for the fixed baseline, corresponding to a reduction of 43.39%. Additional simulations under Federal Test Procedure (FTP-75) and US06 Supplemental Federal Test Procedure (US06) show fuel-consumption reductions of 38.85% and 1.20%, respectively, relative to the baseline. These results demonstrate the potential of adaptive generator-torque modulation to reduce fuel consumption, although the magnitude of the benefit varies with driving conditions. These results demonstrate the potential of adaptive generator-torque modulation to reduce fuel consumption while regulating battery SOC within the prescribed operating range, with the magnitude of fuel savings varying across driving cycles.

Key words**:** energy management strategy, fuel consumption, generator torque control, MATLAB/Simulink, power-split hybrid electric vehicle, state of charge

This paper has been accepted for publication in the AEE journal. This is the version, which has not been fully edited and content may change prior to final publication.
Citation information: DOI 10.24425/aee.2027.8065

1. Introduction

The growing demand for transport services, together with increasingly stringent environmental regulations, has stimulated the development of electric and hybrid vehicle technologies aimed at reducing fuel consumption and greenhouse gas emissions. Hybrid electric vehicles (HEVs) provide an effective combination of the energy density of an internal combustion engine and the efficiency of an electric motor. Fundamental principles of hybrid vehicle energy management were established by Onori *et al*. [1] and Sciarretta and Guzzella [2]. They demonstrated the importance of supervisory control in improving fuel economy. Similarly, Guzzella and Sciarretta [3] and Chan [4] discussed coordinated power sharing and the development of electric and hybrid vehicle technologies, while Ehsani *et al*. [5] presented comprehensive analyses of hybrid powertrain architectures and control strategies.

Considerable research has been devoted to developing efficient EMSs for HEVs. Han *et al*. [6] proposed a real-time energy management strategy based on energy prediction for parallel HEVs. Musardo *et al*. [7] developed the adaptive equivalent consumption minimization strategy (A-ECMS), in which the equivalence factor is adjusted to improve fuel economy. Pisu and Rizzoni [8] compared supervisory control strategies and discussed the trade-off between computational complexity and fuel efficiency. Mittal and Shah [9] reviewed the evolution of HEV energy management technologies, while Liu *et al*. [10] investigated imitation reinforcement learning for adaptive energy management under dynamic driving conditions.

Recent studies have increasingly explored predictive, adaptive, and coordinated control methods for electrified powertrains. Zhou *et al*. [11] combined model predictive control (MPC) with rule-based supervision for a plug-in hybrid vehicle equipped with a hybrid energy storage system. A multi-horizon MPC was used by Hu *et al*. [12], which combines the control of the powertrain and its cooling. Optimal energy management of series HEV, in which there is an engine start-stop control strategy was examined by Chen *et al*. [13], whereas Accurso *et al*. [14] and Jungen *et al*. [15] have considered real-time and rule-based EMSs in hybrid vehicles. The assessment of hybrid powertrain architectures based on fuel efficiency and battery longevity was made by Anselma *et al*. [16]. The fuel-optimal control of power-split and gear-shifting methods was considered by Ritzmann *et al*. [17] and the coordination of energy management and mode-transition losses in input-split HEV was presented by Biswas *et al*. [18].

Among different HEV powertrain architectures the power-split one has unique features due to the combination of mechanical and electrical power distribution through a planetary gearbox. Liu and Peng [19] developed a dynamic model and control strategy for power-split hybrid vehicles. The optimal control problem in order to reduce the energy consumption of the power-split hybrid powertrains was considered by Zhang *et al*. [20] and Zou *et al*. [21] have been studying the modeling and energy management of the power-split HEVs. Energy management based on MPC and double Q-learning methods has been applied to power-split plug-in HEVs by Chen *et al*. [22].

Related research has also examined complementary aspects of energy management and electrified powertrain operation. Khadhraoui *et al*. [24] investigated energy management for a

Early Access

This paper has been accepted for publication in the AEE journal. This is the version, which has not been fully edited and content may change prior to final publication.
Citation information: DOI 10.24425/aee.2027.8065

hybrid electric vehicle, while Unni and Thale [25] studied energy consumption analysis for predicting residual battery energy in electric vehicles. Reddy and Vijaya Kumar [26] examined a hybrid energy storage system for an electric vehicle drive system. Biswas and Emadi [27] reviewed energy management systems for electrified powertrains and discussed emerging research directions. Wang *et al*. [28] investigated hybrid modelling and predictive energy management for a power-split HEV. At the component-control level, Paplicki *et al*. [29] presented simulation and experimental results for a hybrid electric machine employing a novel flux-control strategy. Bena *et al*. [30] investigated an electric vehicle charging management system for an industrial zone, addressing the complementary issue of energy management at the charging-system level.

Despite these developments, the design of computationally efficient supervisory EMSs for PS-HEVs remains challenging because the engine, generator, motor, planetary gear system, and battery are mechanically and electrically coupled. The selection of engine operating conditions and the allocation of power between the mechanical and electrical paths must therefore be coordinated with the battery SOC and instantaneous traction demand. In particular, there is scope to investigate the explicit use of generator torque as a supervisory control variable in a rule-based PS-HEV EMS, together with SOC regulation and load-dependent adaptation.

Motivated by this requirement, this paper proposes an adaptive generator-torque-driven EMS with integrated SOC regulation for a PS-HEV. Unlike conventional rule-based approaches that primarily regulate engine and motor power sharing, the proposed method uses generator torque as a principal supervisory control variable while considering vehicle speed, traction power demand, and battery SOC. The objective is to reduce fuel consumption while regulating battery SOC within the prescribed operating range. The strategy is implemented in a MATLAB/Simulink-based PS-HEV model and evaluated primarily under the UDDS driving cycle, with additional simulations conducted under FTP-75 and US06. Four EMS strategies are compared using fuel consumption and battery SOC behaviour as performance measures. Under UDDS, the proposed Case 4 achieves a 43.39% reduction in simulated fuel consumption relative to the baseline Case 1. The additional drive-cycle results are used to assess how the fuel-saving performance varies under different driving conditions. The main contributions of this research are as follows:

- An adaptive energy management scheme in which generator torque acts as a principal supervisory variable for regulating energy transfer in a PS-HEV.
- The incorporation of load dependent generator torque control into an SOC based supervisory scheme to coordinate mechanical and electrical energy flows.
- Performance evaluation of the developed approach using a MATLAB/Simulink PS-HEV model, with UDDS as the primary driving cycle and additional evaluation under FTP-75 and US06.
- Comparative evaluation of fixed, speed based, speed-SOC-load adaptive, and proposed SOC protected adaptive control strategies.
- Quantitative comparison of fuel consumption and battery SOC variation among the evaluated EMS strategies.

Early Access

This paper has been accepted for publication in the AEE journal. This is the version, which has not been fully edited and content may change prior to final publication.
Citation information: DOI 10.24425/aee.2027.8065

The remainder of this paper is organized as follows. Section 2 presents the PSHEV model and its configuration. Section 3 describes the EMSs, and Section 4 details the proposed adaptive EMS. Section 5 presents the simulation results and discussion, followed by the conclusions in Section 6.

2. Powersplit HEV modeling

2.1. System configuration

The PS-HEV considered here has a planetary gear set that connects the engine, the generator, and the traction motor together. The planetary gear set enables simultaneous mechanical and electrical power transmission, allowing the engine power to be split between the two transmission paths. With the setup chosen in this analysis, the engine is attached to the carrier, the generator to the sun gear, and the motor to the ring gear that drives the wheels. With such a combination, the engine power can be transmitted through two routes – mechanically to the wheels and electrically via the generator and the motor. In this configuration, the generator performs a dual role in the power split mechanism by converting mechanical power into electrical power and influencing the operating point of the planetary gear set. Figure 1 shows the PS-HEV architecture with the planetary gear coupling between the engine (carrier), generator (sun gear), and motor (ring gear).

Early Access

2.2. Planetary gear relationships

The kinematic relationship of the planetary gear set is expressed in (1), where ω_r, ω_s and ω_c represent the angular speeds of the ring gear, sun gear, and carrier, respectively, and N_s and N_r denote the number of teeth of the sun and ring gears.

$$\omega_r = \omega_c + \frac{N_S}{N_r(\omega_c - \omega_S)}. \tag{1}$$

Under the ideal, lossless planetary gear assumption, the torque relationship follows conservation of power and is expressed by (2), where T_c, T_s, and T_r are the torques at the carrier, sun gear, and ring gear, respectively. These relationships illustrate the inherent coupling between mechanical and electrical components in the power-split architecture.

$$T_c\omega_c + T_s\omega_s + T_r\omega_r = 0. \tag{2}$$

This paper has been accepted for publication in the AEE journal. This is the version, which has not been fully edited and content may change prior to final publication.
Citation information: DOI 10.24425/aee.2027.8065

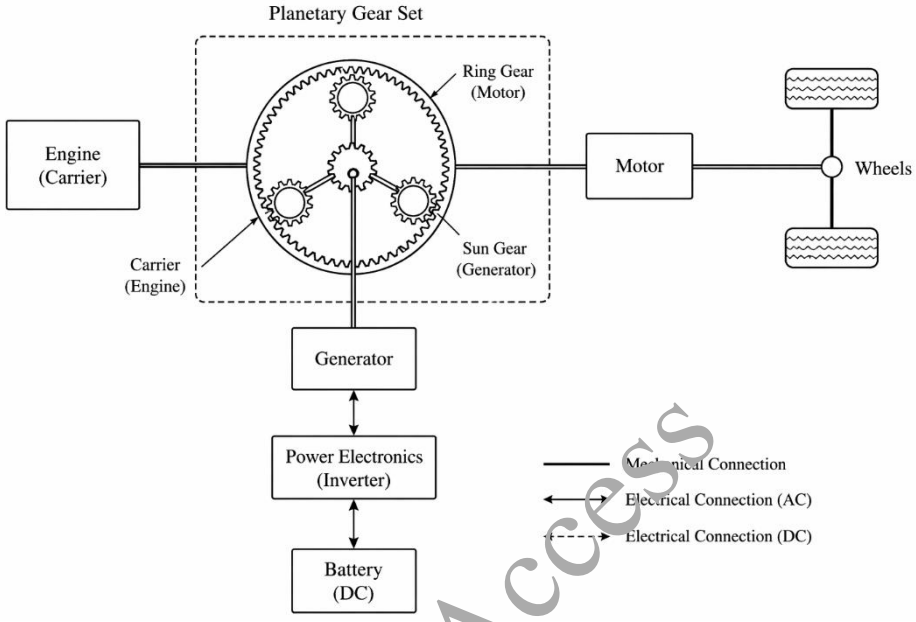


Fig. 1. Power-split HEV architecture showing the planetary gear coupling between the engine (carrier), generator (sun gear), and motor (ring gear)

Early Access

2.3. Power flow characteristics

The total engine power is divided between mechanical and electrical power paths through the planetary gear set. The generator power is expressed in (3), where T_{gen} and ω_{gen} denote the generator torque and angular speed, respectively. A negative generator torque convention is adopted in this work; therefore, for positive generator speed, negative P_{gen} represents mechanical power absorbed by the generator and converted into electrical power.

$$P_{\text{gen}} = T_{\text{gen}} \cdot \omega_{\text{gen}} \,. \tag{3}$$

2.4. Battery model

Equation (4) represents the battery power, where V_{oc} is the SOC dependent open circuit voltage and I_{bat} is the battery current. The SOC dynamics are represented by (5), where Q_{bat} denotes the battery capacity. The battery model used in the simulation has a nominal voltage of 201.6 V, a capacity of 150 Ah, and internal resistances of 0.03 Ω during both charging and discharging. The initial battery charge is 100 Ah, corresponding to an initial SOC of 0.6667, and the battery operating temperature is set to 298.15 K.

$$P_{\text{bat}} = V_{\text{oc}}(\text{SOC}) \cdot I_{\text{bat}} \,, \tag{4}$$

$$\frac{\text{d(SOC)}}{\text{d}t} = \frac{I_{\text{bat}}}{Q_{\text{bat}}}. \tag{5}$$

This paper has been accepted for publication in the AEE journal. This is the version, which has not been fully edited and content may change prior to final publication.
Citation information: DOI 10.24425/aee.2027.8065

The main battery parameters used in the PS-HEV simulation are summarized in Table 1.

Table 1. Battery parameters

Parameter	Value	Unit
Nominal battery voltage	201.6	V
Battery capacity, Q_{bat}	150	Ah
Discharge internal resistance	0.03	Ω
Charge internal resistance	0.03	Ω
Initial battery charge	100	Ah
Initial state of charge (SOC)	0.6667	–
Battery operating temperature	298.15	K

The total traction power requirement P_{req} is represented as the sum of the mechanical power delivered to the wheels, P_{wheel}, and the drivetrain and conversion losses, P_{loss}, as given in (6).

$$P_{req} = P_{wheel} + P_{loss}. \tag{6}$$

From a control theoretic perspective, generator torque is an important decision variable because it affects both the electrical power generation and the engine operating point. Variation of generator torque changes the proportion of engine power converted into electrical power and thereby influences engine speed and loading. Unlike series HEVs, in which the engine is mechanically decoupled from the wheels, and parallel HEVs, in which engine and motor torques are directly combined at the mechanical output, the power split configuration involves inherent coupling among the speeds and torques of the engine, generator, and motor. Consequently, the energy management problem involves coordinated control of the mechanical and electrical subsystems. The objective is therefore to determine suitable generator torque and engine speed commands that reduce fuel consumption while maintaining the battery SOC within acceptable limits. This forms the basis of the adaptive energy management method presented in the next section.

The principal vehicle and electrical-drive parameters used in the PS-HEV model are summarized in Table 2. The planetary gear, engine, generator, and drivetrain parameters are specified according to the implemented simulation model.

Table 2. PS-HEV model parameters

Parameter	Symbol	Value	Unit
Vehicle mass	M_v	1 200	kg
Rolling resistance coefficient	C_{rr}	0.01	–
Aerodynamic drag coefficient	C_d	0.30	–

Early Access

This paper has been accepted for publication in the AEE journal. This is the version, which has not been fully edited and content may change prior to final publication.
Citation information: DOI 10.24425/aee.2027.8065

Frontal area	A_f	1.40	m²
Air density	ρ	1.225	kg/m³
Gravitational acceleration	g	9.81	m/s²
Wheel radius	r_w	0.30	m
Maximum power limit	$P_{\max}$	50	kW
Maximum torque limit	$T_{\max}$	400	N·m
Ring-Planet teeth ratio	N_r/N_p	1.3	–

3. Energy management strategies

Early Access

3.1. Overview

The PS-HEV considered in this study employs a planetary gear system to couple the internal combustion engine, generator, and traction motor. Owing to this mechanical and electrical coupling, the supervisory EMS must coordinate engine-speed and generator-torque commands while accounting for vehicle operating conditions and battery SOC.

To evaluate the influence of supervisory control complexity on vehicle performance, four EMS strategies are implemented and compared. These strategies progressively incorporate vehicle-speed dependence, SOC-based regulation, traction-load adaptation, and additional supervisory protection. Case 1 provides a fixed baseline, Case 2 introduces speed-dependent control, Case 3 incorporates speed, SOC, and traction power demand, and Case 4 introduces the proposed SOC-protected adaptive control strategy. The mathematical formulation and implementation details of the proposed Case 4 controller are presented in Section 4.

3.2. Development of EMS cases

Four supervisory control strategies are implemented to investigate the effect of progressively increasing control complexity on PS-HEV performance. The strategies differ in their use of vehicle speed, battery SOC, traction power demand, and additional operating constraints.

3.2.1 Case 1: fixed baseline strategy:

Case 1 serves as the baseline strategy. The engine-speed reference is fixed at 2 000 rpm, and the generator-torque reference is set to −3 N.m. These commands do not adapt to vehicle speed, battery SOC, or traction power demand. This case provides a reference for evaluating the effects of introducing additional supervisory control features.

3.2.2. Case 2: speed based strategy:

Case 2 introduces vehicle-speed-dependent control. The engine-speed and generator-torque references are determined from the instantaneous vehicle speed, (v), according to the supervisory functions (7) and (8). Here ω_e^* is the reference engine speed and T_g^* is the reference generator

This paper has been accepted for publication in the AEE journal. This is the version, which has not been fully edited and content may change prior to final publication.
Citation information: DOI 10.24425/aee.2027.8065

torque. The schedules use three vehicle-speed regions: below 10 mph, from 10 to 35 mph, and 35 mph or above. The corresponding reference values vary with vehicle speed within each region. Although this strategy responds to changes in vehicle speed, it does not explicitly use battery SOC or traction power demand to adjust the supervisory commands.

$$\omega_e^* = f(v), \tag{7}$$
$$T_g^* = f(v).$$

3.2.3. Case 3: speed-SOC-load adaptive strategy:

Case 3 extends the speed-based strategy by incorporating battery SOC and traction power demand. The supervisory controller uses vehicle speed, SOC, and required traction power to adjust the engine speed and generator torque references according to the instantaneous driving condition. The corresponding control relationships are represented by (9) and (10), where v denotes vehicle speed, SOC denotes battery state of charge, and P_{req} denotes required traction power. Compared with Case 2, this strategy considers both battery energy status and load demand. However, it uses a different SOC reference and operating band from the proposed Case 4 strategy, and its supervisory rules do not include all the additional SOC protection and low speed constraints used in Case 4.

$$\omega_e^* = f_3(v, \mathrm{SOC}, P_{\mathrm{req}}), \tag{9}$$
$$T_g^* = g_3(v, \mathrm{SOC}, P_{\mathrm{req}}). \tag{10}$$

3.2.4. Case 4: proposed SOC protected adaptive strategy:

Case 4 is the proposed adaptive EMS. It builds on the speed–SOC–load strategy by incorporating continuous SOC-error feedback, load-dependent corrections, adaptive engine-speed scheduling, generator-torque modulation, and additional operating constraints. The controller uses an SOC reference of 0.62, with lower and upper SOC thresholds of 0.58 and 0.66, respectively. It also applies speed-dependent base schedules, load-dependent corrections, a low-speed generator-torque constraint, and command saturation limits.

The proposed controller determines the engine-speed and generator-torque references using vehicle speed, SOC deviation, and required traction power. Its detailed mathematical formulation, parameter values, and control sequence are presented in Section 4. The principal features of the four strategies are summarized in Table 3.

Table 3. Comparison of the four EMS strategies

Control feature	**Case 1: fixed baseline**	**Case 2: speed-based**	**Case 3: speed-SOC-load adaptive**	**Case 4: proposed SOC-protected adaptive**
Vehicle-speed dependence	No	Yes	Yes	Yes
SOC-based control	No	No	Yes	Yes

Early Access

This paper has been accepted for publication in the AEE journal. This is the version, which has not been fully edited and content may change prior to final publication.
Citation information: DOI 10.24425/aee.2027.8065

Load adaptation	No	No	Yes	Yes
Continuous SOC-error-based correction	No	No	No	Yes
SOC threshold-based protection	No	No	No	Yes
Low-speed torque constraint	No	No	No	Yes

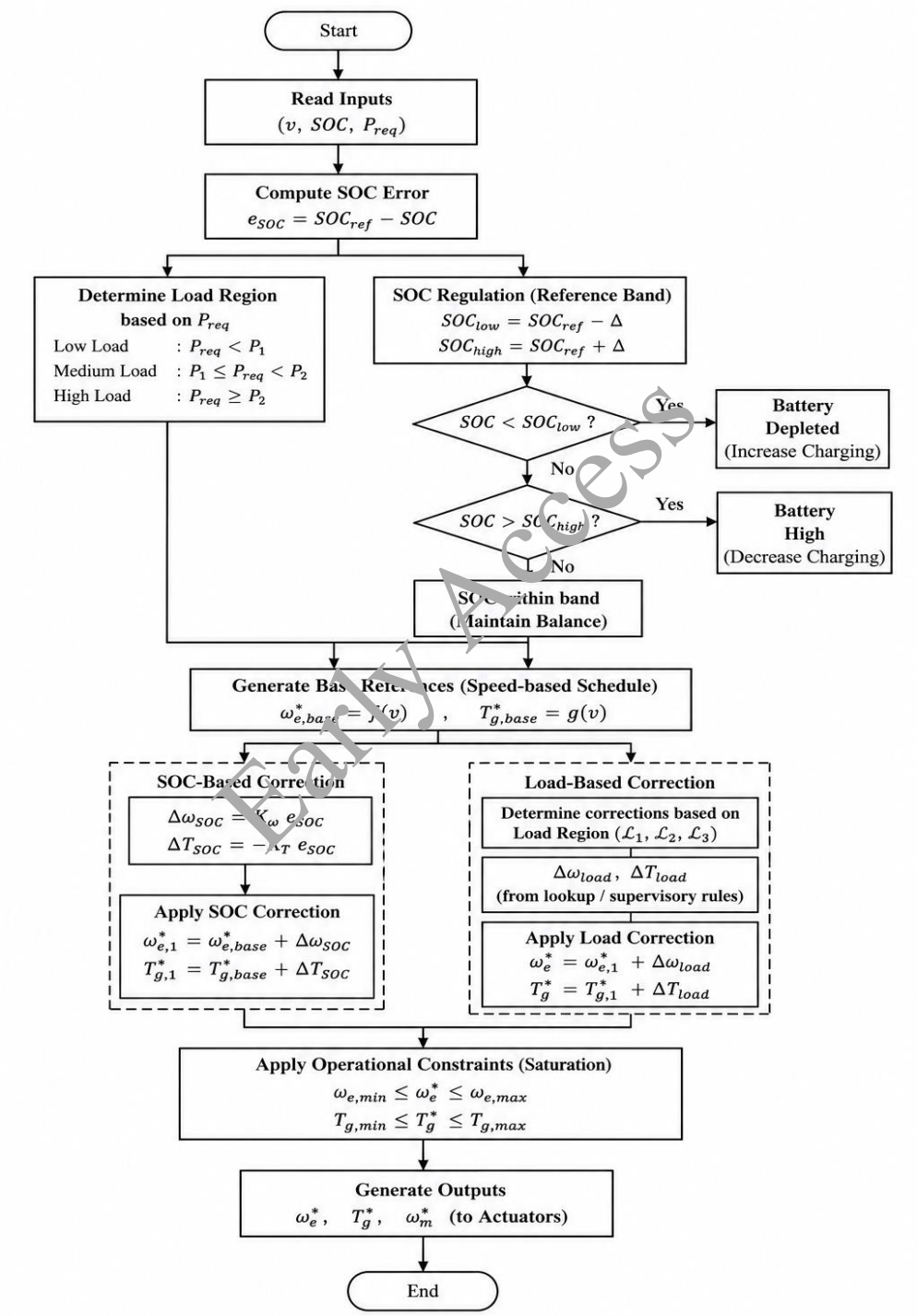
4. Proposed adaptive energy management strategy

4.1. Control objectives

The primary objective of the proposed EMS is to reduce fuel consumption while regulating battery SOC during vehicle operation. The controller coordinates the engine, generator, traction motor, and battery according to vehicle speed, required traction power, and battery SOC. Generator torque is used as a principal supervisory control variable because it influences electrical power generation and the distribution of power through the planetary gear system. The proposed strategy combines speed-dependent scheduling, SOC-error feedback, load-dependent corrections, and operating constraints within a rule-based supervisory controller. The control structure of the proposed EMS is illustrated in Fig. 2.

Early Access

This paper has been accepted for publication in the AEE journal. This is the version, which has not been fully edited and content may change prior to final publication.
Citation information: DOI 10.24425/aee.2027.8065



Early Access

This paper has been accepted for publication in the AEE journal. This is the version, which has not been fully edited and content may change prior to final publication.
Citation information: DOI 10.24425/aee.2027.8065

Fig. 2. Flowchart of the proposed adaptive energy management strategy for the power-split HEV

4.2. Overview

The proposed adaptive EMS uses vehicle speed (v), battery SOC, and required traction power (P_{req}) as its principal inputs. Based on these inputs, the controller first determines nominal engine-speed and generator-torque references from predefined speed-dependent schedules. It then applies corrections based on SOC deviation and traction-load classification. Finally, the resulting commands are constrained by the specified engine-speed and generator-torque limits. This sequence integrates speed-based scheduling, SOC feedback, load adaptation, and supervisory protection into a single rule-based control framework.

4.3. Input variables

At each interval of the control cycle, the supervisory controller takes the measurement of the instantaneous speed of the vehicle (v), SOC of the battery, and the required traction power (P_{req}). The three parameters are essential in determining the operating state of the vehicle. The speed of the vehicle is important in determining the base operating state of the engine generator unit, while the SOC determines the level of energy available.

4.4. Load classification

The required traction power is classified into three operating regions using two supervisory thresholds, P_1 and P_2, as expressed in (11). For the proposed Case 4 controller, the thresholds are $P_1 = 8$ kW and $P_2 = 20$ kW. The load region determines the additional correction applied to the nominal engine speed and generator torque references. For load classification, the non-negative traction power demand is defined as $P_{\mathrm{req}} = \max(P_{\mathrm{dem}}, 0)$, where P_{dem} is the instantaneous traction power requirement. This ensures that negative traction power does not produce a negative load classification.

The load region is defined as follows:

$$L(P_{\mathrm{req}}) = \begin{cases} L_1 & P_{\mathrm{req}} < P_1 \\ L_2 & P_1 \le P_{\mathrm{req}} < P_2 \\ L_3 & P_{\mathrm{req}} \ge P_2 \end{cases}. \tag{11}$$

4.5. SOC regulation

Battery SOC regulation is implemented using a reference SOC and predefined lower and upper limits. For the proposed Case 4 strategy, the reference SOC is $\mathrm{SOC}_{\mathrm{ref}} = 0.62$, while the lower and upper limits are $\mathrm{SOC}_{\mathrm{low}} = 0.58$ and $\mathrm{SOC}_{\mathrm{high}} = 0.66$, respectively. The SOC error is calculated using (14). This error provides a continuous correction to the engine speed and generator torque references. Additional threshold-based corrections are applied when SOC falls below the lower limit or rises above the upper limit.

$$\mathrm{SOC}_{\mathrm{low}} = \mathrm{SOC}_{\mathrm{ref}}\, \Delta, \tag{12}$$

$$\mathrm{SOC}_{\mathrm{high}} = \mathrm{SOC}_{\mathrm{ref}} + \Delta, \tag{13}$$

Early Access

This paper has been accepted for publication in the AEE journal. This is the version, which has not been fully edited and content may change prior to final publication.
Citation information: DOI 10.24425/aee.2027.8065

$$e_{\mathrm{SOC}} = \mathrm{SOC}_{\mathrm{ref}}\ \mathrm{SOC}. \tag{14}$$

When SOC falls below the lower limit, the controller applies additional engine speed and generator torque corrections intended to increase engine involvement and electrical energy generation. When SOC exceeds the upper limit, the controller reduces the engine speed reference and relaxes the generator torque command to reduce charging demand. The exact corrections and their numerical values are specified in Section 4.7.

4.6. Base engine and generator scheduling

The proposed energy management strategy first determines the nominal operating point of the engine–generator set based on vehicle speed. The nominal engine speed and generator torque references are selected according to predefined speed dependent scheduling rules. These reference values provide the baseline for subsequent adaptation based on battery SOC and traction power demand. This approach enables the controller to adjust the engine - generator operating point according to the vehicle's operating conditions while maintaining a structured supervisory control framework. The detailed scheduling rules are implemented in the MATLAB function used for the simulations.

4.7. Adaptive engine speed scheduling

The engine speed reference is adaptively modified according to the battery SOC and the instantaneous traction load. The reference speed of the engine is provided using Eq. (15), where $\omega_{e,\ \mathrm{base}}$ refers to the base engine speed profile, whereas $\Delta\omega_{\mathrm{SOC}}$ and $\Delta\omega_{\mathrm{load}}$ refer to the corrections made due to the SOC and traction load respectively. These corrections ensure that the engine's operating point is appropriately varied according to changes in battery energy level and power requirement of the vehicle. The reference thus generated will be kept within the allowed engine operation range.

$$\omega_e^* = \omega_{e,\mathrm{base}} + \Delta\omega_{\mathrm{SOC}} + \Delta\omega_{\mathrm{load}}\ . \tag{15}$$

4.8. Adaptive generator torque modulation

Generator torque is used as a key supervisory control variable because it influences electrical power generation and indirectly affects the engine operating point through the planetary gear system. The reference generator torque is determined using (16), where $T_{g,\mathrm{base}}$ denotes the nominal generator torque schedule, while ΔT_{SOC} and ΔT_{load} represent the corrections associated with battery SOC and traction load, respectively. These modifications help the controller match the generator performance with the battery energy condition and the vehicle power requirement. This results in the generated torque reference being within the permissible limits of generator operation.

$$T_g^* = T_{g,\mathrm{base}} + \Delta T_{\mathrm{SOC}} + \Delta T_{\mathrm{load}}\ . \tag{16}$$

The convention for negative torque used in this research work refers to the fact that the generator takes in mechanical energy from the engine and produces electrical energy. Thus, when

Early Access

This paper has been accepted for publication in the AEE journal. This is the version, which has not been fully edited and content may change prior to final publication.
Citation information: DOI 10.24425/aee.2027.8065

the speed of the generator is positive, negative generator torque refers to negative mechanical power, which implies that the generator is operational.

4.9. Operational constraints

Constraints are applied to the control signals so as to allow practical implementation of the control strategy and ensure stable control. The engine speed control signal is constrained according to Eq. (17), whereas the generator torque control signal is constrained based on Eq. (18).

$$\omega_{e,\min} \leq \omega_e^* \leq \omega_{e,\max}, \tag{17}$$

$$T_{g,\min} \leq T_g^* \leq T_{g,\max}. \tag{18}$$

The principal numerical parameters and operating limits of the proposed Case 4 controller are summarized in Table 4 to support reproducibility of the simulation results.

Table 4. Controller parameters for the EMS

Parameter	Symbol	Value	Unit
Reference SOC	SOC_{ref}	0.62	–
Lower SOC limit	SOC_{low}	0.58	–
Upper SOC limit	SOC_{high}	0.66	–
Low-load threshold	P_1	8	kW
Medium/high-load threshold	P_2	20	kW
Lower vehicle-speed breakpoint	v_1	10	mph
Upper vehicle-speed breakpoint	v_2	35	mph
Low-speed torque-protection threshold	v_{min}	8	mph
SOC-error correction gain for engine speed	K_{speed}	180	rpm per unit SOC error
SOC-error correction gain for generator torque	K_{torque}	0.8	N·m per unit SOC error
Minimum engine-speed reference	–	0	rpm
Maximum engine-speed reference	–	2 800	rpm
Generator-torque command limits	–	−4 to 0	N·m
Low-speed generator-torque constraint	–	$T_g \geq -2$	N·m

Early Access

4.10. Control sequence

The proposed adaptive EMS operates according to the following sequence:

1. Acquire the instantaneous vehicle speed (v), battery SOC, and required traction power (P_{req}).

This paper has been accepted for publication in the AEE journal. This is the version, which has not been fully edited and content may change prior to final publication.
Citation information: DOI 10.24425/aee.2027.8065

2. Classify the operating condition into low, medium, or high load regions.
3. Compute the SOC error with respect to the reference SOC.
4. Generate the nominal engine speed and generator torque references based on vehicle speed.
5. Apply SOC dependent adaptive corrections and load dependent supervisory corrections.
6. Enforce the operational constraints on engine speed and generator torque.
7. Provide the final engine speed, generator torque, and motor speed references to the corresponding drivetrain subsystems.

4.11. Summary

The proposed adaptive EMS integrates vehicle speed, battery SOC, and required traction power within a hierarchical supervisory control framework to coordinate the operation of the engine, generator, motor, and battery. By combining adaptive engine speed scheduling, generator torque modulation, SOC regulation, and load aware supervisory corrections, the controller coordinates power distribution within the planetary gear-based power split architecture. The proposed strategy aims to improve fuel economy while maintaining battery SOC within the desired operating range and supporting stable vehicle operation under varying driving conditions.

Early Access

5. Results and discussion

5.1. Simulation setup

The proposed EMS was implemented in MATLAB/Simulink using a PS-HEV model. The vehicle is evaluated using the standard UDDS drive cycle, with a simulation duration of 1370 s. UDDS driving cycle was adopted to be the major driving cycle since it reflects the characteristics of urban traffic which consists of numerous stops, starts and deceleration. This cycle was chosen to evaluate the energy management capability of power-split HEV during city driving cycle. The UDDS driving cycle is widely used in light-duty vehicle testing. In order to expand the simulation to different driving situations besides the urban situation, the proposed EMS was simulated using both FTP-75 and US06 driving cycles as well. FTP-75 incorporates the UDDS pattern with a repeated initial segment after the soak segment, hence, FTP-75 provides the extended driving cycle, on the other hand, US06 provides the aggressive driving cycle with more acceleration requests. Therefore, the UDDS driving cycle remained as the main testing cycle, while FTP-75 and US06 were used to compare different fuel saving performances in different driving cycles.

The overall driving distance was calculated through integrating the vehicle speed throughout the driving cycle. Based on the implemented UDDS speed-time pattern, the distance that is obtained is 12.35 km. Fuel consumption calculation was performed over the whole driving cycle and then the total fuel consumption was normalized by the driving distance in order to obtain fuel consumption in kg/100 km and g/km.

This paper has been accepted for publication in the AEE journal. This is the version, which has not been fully edited and content may change prior to final publication.
Citation information: DOI 10.24425/aee.2027.8065

For all cases, the initial SOC of the battery was defined as 0.6667. Four energy management strategies were investigated as follows:

– Case 1: Fixed baseline control,
– Case 2: Speed-based control,
– Case 3: Speed-SOC-load adaptive control,
– Case 4: Proposed SOC- protected load aware control.

5.2. SOC behavior

Figure 3 shows the SOC fluctuations for the four different control schemes. In all of the above control strategies, there is a decline in the SOC level over the driving cycle, although this change is of varying magnitude depending on the case. The minimum SOC level at the end of the cycle is seen for Case 3, while Case 1 has the maximum SOC level at the end of the driving cycle. Case 4 has achieved slightly less reduction in the SOC level compared to Case 3.

Figure 4 shows the final SOC levels for the four control schemes. It can be observed that although Case 1 has the highest SOC level, it has the highest fuel consumption level as well. Case 4 has shown the least fuel consumption rate among all the analyzed cases, with slightly higher SOC level than Case 3.

The goal of SOC regulation in the current study is to regulate the battery energy usage according to the specified range of operation to minimize the fuel consumption rate. Therefore, the difference in the final SOC value between the four cases cannot be viewed as an indication of the failure of the regulation objective. The SOC trajectories should be considered together with fuel consumption when evaluating the performance of each strategy.

Early Access

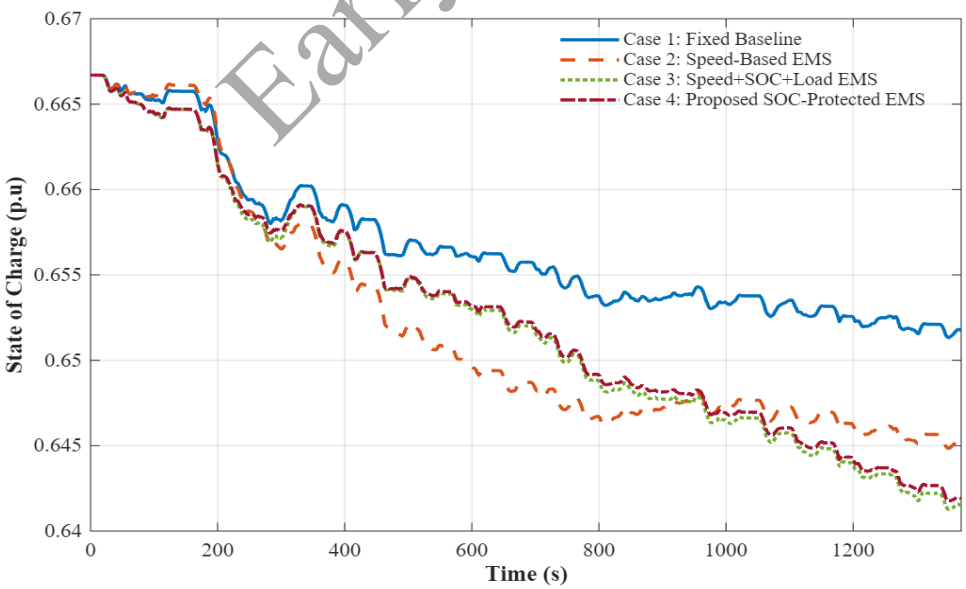


Fig. 3. SOC variation for different energy management strategies under the driving cycle

This paper has been accepted for publication in the AEE journal. This is the version, which has not been fully edited and content may change prior to final publication.
Citation information: DOI 10.24425/aee.2027.8065

5.3. Fuel consumption analysis

The fuel consumption of the four strategies is compared in Fig. 5. The proposed Case 4 achieves the lowest fuel consumption of 0.1249 kg, compared with 0.2206 kg for Case 1. This corresponds to a 43.39% reduction in fuel consumed over the UDDS cycle relative to the baseline strategy. To provide a distance-normalized comparison, fuel consumption was also expressed in kg/100 km and g/km using the calculated UDDS distance of 12.35 km. For the proposed Case 4, the total fuel consumed was 0.1249 kg, corresponding to a normalized fuel consumption of 1.0112 kg/100 km (10.11 g/km). This metric complements the total fuel consumed over the drive cycle and facilitates comparison with results reported using distance-based fuel consumption measures.

The proposed controller is designed to reduce fuel consumption while regulating battery SOC, rather than forcing identical final SOC values for all strategies. Accordingly, fuel consumption and SOC behavior are considered together when assessing the effectiveness of the proposed EMS.

Early Access

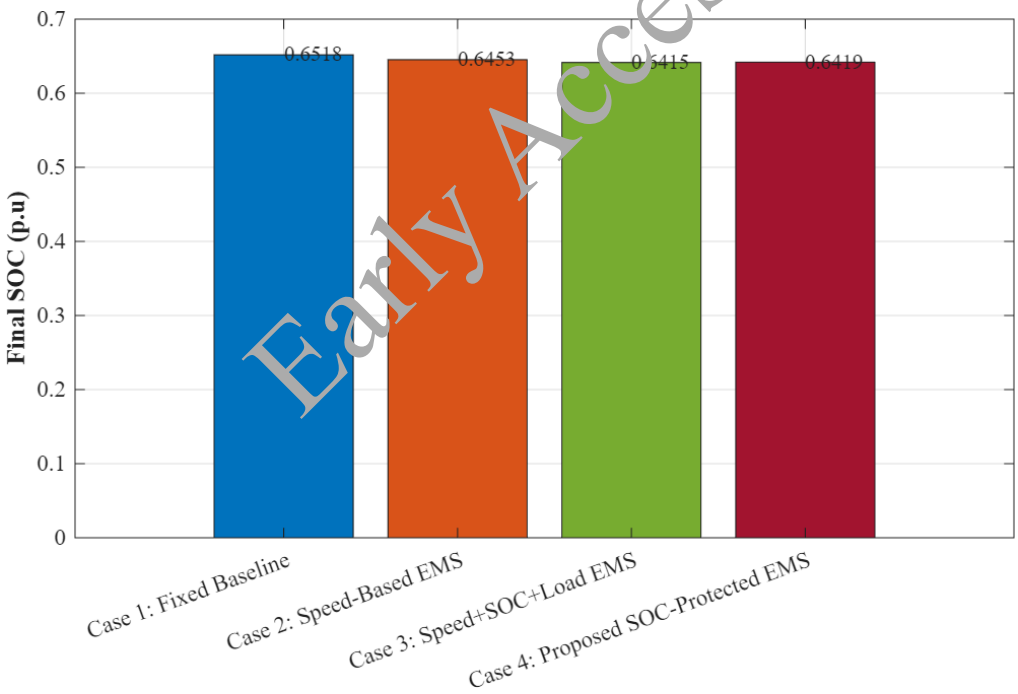


Fig. 4. Final SOC values for different energy management strategies

This paper has been accepted for publication in the AEE journal. This is the version, which has not been fully edited and content may change prior to final publication.
Citation information: DOI 10.24425/aee.2027.8065

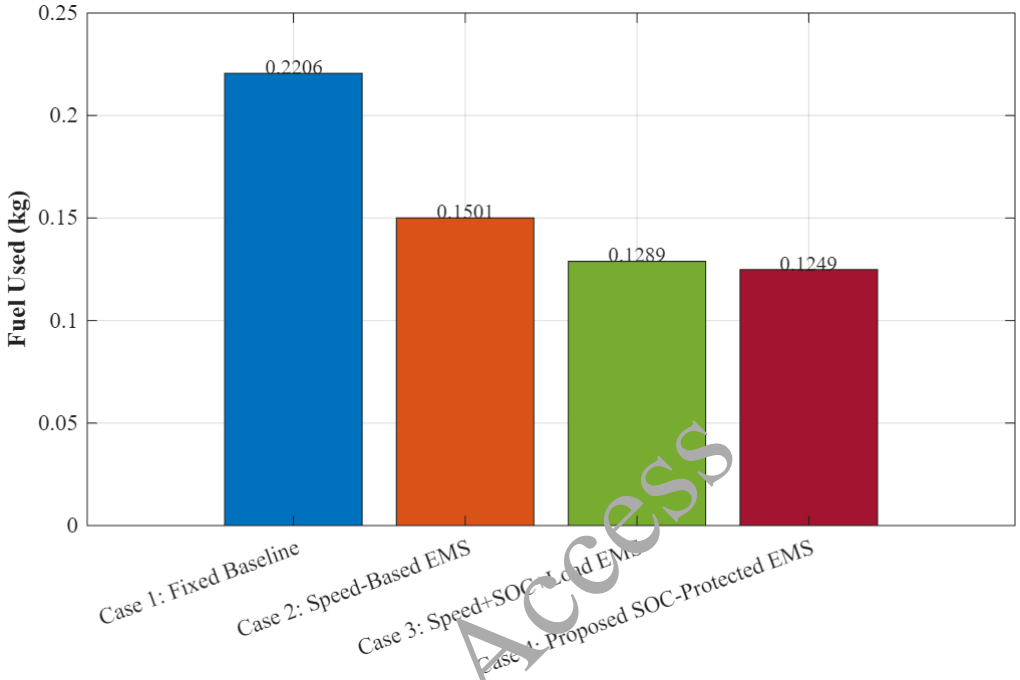


Fig. 5. Comparison of fuel consumption for the evaluated energy management strategies

Early Access

5.4. Quantitative performance comparison

Table 5 compares the fuel consumption and battery SOC variation of the four EMS strategies. Case 4 achieves the lowest fuel consumption of 0.1249 kg, compared with 0.1289 kg for Case 3 and 0.2206 kg for Case 1. The final SOC of Case 4 is 0.6419, slightly higher than the 0.6415 obtained with Case 3. These results show that Case 4 provides the lowest simulated fuel consumption among the evaluated strategies while exhibiting slightly better final SOC retention than Case 3.

To further evaluate the proposed EMS under different driving conditions, simulations were also conducted using the FTP-75 and US06 drive cycles. The proposed Case 4 reduced fuel consumption from 17.86 to 10.11 g/km under UDDS, from 16.69 to 10.21 g/km under FTP-75, and from 8.46 to 8.36 g/km under US06, relative to the fixed baseline (Case 1). These results correspond to fuel-consumption reductions of 43.39%, 38.85%, and 1.20%, respectively. The results indicate that the fuel-saving performance of the proposed EMS varies with the driving cycle and its associated operating conditions. Figure 6 compares the SOC reduction for the evaluated strategies. The results show that the proposed strategy achieves the lowest measured fuel consumption among the four cases while slightly improving SOC retention relative to Case 3. However, the final SOC of Case 4 remains below that of the baseline strategy, and the comparison does not establish equivalent battery energy depletion across all cases.

This paper has been accepted for publication in the AEE journal. This is the version, which has not been fully edited and content may change prior to final publication.
Citation information: DOI 10.24425/aee.2027.8065

Table 5. Quantitative performance comparison

EMS strategy	Initial SOC	Final SOC	SOC drop	Fuel consumption (kg)	Fuel consumption (kg/100 km)	Fuel reduction w.r. to Case 1 (%)
Case 1: fixed baseline	0.6667	0.6518	0.0149	0.2206	1.7860	0.00
Case 2: speed-based	0.6667	0.6453	0.0214	0.1501	1.2150	32.00
Case 3: speed-SOC-load adaptive	0.6667	0.6415	0.0252	0.1289	1.0436	41.56
Case 4: proposed SOC-protected load aware	0.6667	0.6419	0.0248	0.1249	1.0112	43.39

5.5. Power flow analysis

The generator and battery power profiles for the proposed strategy are shown in Fig. 7. Under the adopted sign convention, the predominantly negative generator power profile indicates mechanical to electrical energy conversion when the generator operates at positive speed. This behavior is consistent with the generator role in converting mechanical power from the engine into electrical power within the power split architecture.

The generator power sign convention is defined by $P_g = T_g/\omega_g$. For positive generator speed, the negative generator torque translates to negative mechanical power, which means the generator receives mechanical power and turns it into electrical power. The battery power notation is determined with reference to the corresponding Simulink measurement block. In addition, the charging and discharging states are clearly distinguished. The conventions mentioned above are used when analyzing the power diagrams presented in Fig. 7.

From the battery power diagram, it can be seen that there are moments of battery charging and discharge depending on the vehicle's state. These variations depend on the traction power requirements and the work of the generator with the battery.

Early Access

This paper has been accepted for publication in the AEE journal. This is the version, which has not been fully edited and content may change prior to final publication.
Citation information: DOI 10.24425/aee.2027.8065

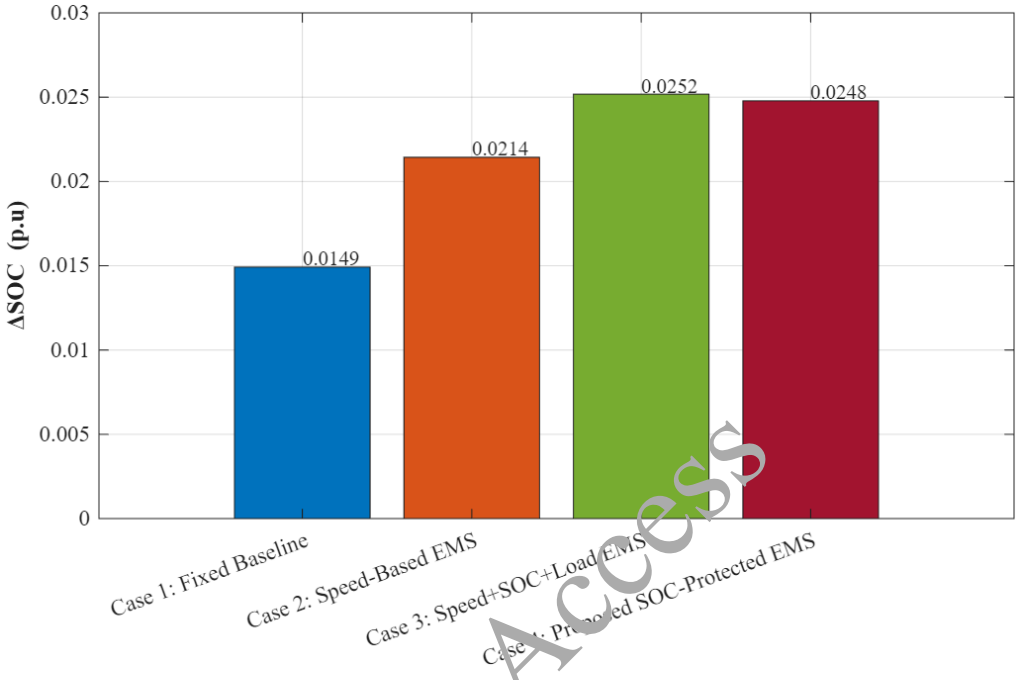


Fig. 6. Comparison of SOC drop for the evaluated energy management strategies

Early Access

5.6. Discussion

The simulation output shows the possibility of using a control algorithm based on the regulation of the generator's torque for decreasing the fuel consumption while sustaining battery SOC. Four cases have been investigated using the identical initial SOC and the UDDS driving cycle. The differences in the final value of the SOC for each case come from different control rules that lead to different ways of operating the engine–generator system and the battery usage. Among these cases, Case 4 uses less fuel and slightly improves the final SOC in comparison with Case 3. The mentioned 43.39% reduction is the measure of difference in fuel consumption in comparison with Case 1; however, the SOC dynamics in this case have been described in the separate paragraph.

Nevertheless, the obtained result is true only for the simulated UDDS cycle and the given model parameters. As the final SOC values differ between cases, the obtained reduction in fuel consumption cannot be interpreted as the equivalent reduction in charge-sustaining mode. Further evaluation using SOC corrected fuel consumption, additional driving cycles, and sensitivity analysis would strengthen the assessment of the proposed strategy. Experimental validation is also required before drawing conclusions about real vehicle performance.

This paper has been accepted for publication in the AEE journal. This is the version, which has not been fully edited and content may change prior to final publication.
Citation information: DOI 10.24425/aee.2027.8065

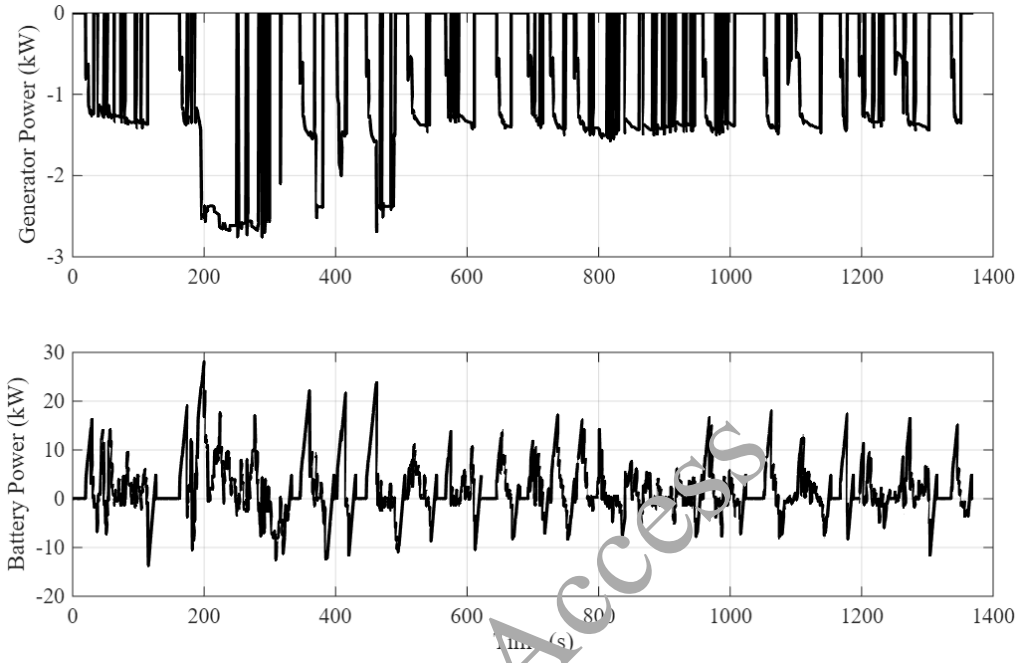


Fig. 7. Generator and battery power profiles for the proposed strategy. Negative generator power indicates conversion of mechanical energy into electrical energy.

Early Access

6. Conclusions

An adaptive energy management algorithm is proposed for a PS-HEV, in which generator torque and battery SOC are used for power-flow regulation. The proposed algorithm considers the coupling introduced by the planetary gear train to coordinate mechanical and electrical power flow. The distribution of engine power between the mechanical and electrical paths is regulated through coordinated generator-torque and engine control based on traction load, vehicle speed, and battery SOC.

The simulation results show that the proposed Case 4 reduces fuel consumption from 0.2206 kg for the baseline Case 1 to 0.1249 kg under the UDDS drive cycle, corresponding to a reduction of 43.39%. Case 4 also reduces fuel consumption relative to Case 3, from 0.1289 kg to 0.1249 kg, while achieving a slightly higher final SOC. Additional evaluations under the FTP-75 and US06 drive cycles show fuel-consumption reductions of 38.85% and 1.20%, respectively, relative to Case 1. These results demonstrate the potential of adaptive generator-torque modulation combined with SOC-based and load-aware supervisory control to improve fuel-consumption performance, although the magnitude of the benefit varies with the driving cycle.

This paper has been accepted for publication in the AEE journal. This is the version, which has not been fully edited and content may change prior to final publication.
Citation information: DOI 10.24425/aee.2027.8065

The proposed strategy employs a rule-based supervisory controller without requiring computationally intensive online optimization. The present evaluation is based on simulation, and the reported fuel-consumption reductions do not account for differences in final battery SOC. Further research should investigate SOC-corrected fuel-consumption assessment, robustness under varying operating conditions, and experimental validation. The integration of predictive or learning-based methods may also improve adaptability and support multi-objective energy management incorporating exhaust emissions and component degradation.

References

[1] Onori S., Serrao L., Rizzoni G., *Hybrid Electric Vehicles: Energy Management Strategies*, Springer (2016), DOI: 10.1007/978-1-4471-6781-5.
[2] Sciarretta A., Guzzella L., *Control of Hybrid Electric Vehicles*, IEEE Control Systems Magazine, vol. 27, no. 2, pp. 60–70 (2007), DOI: 10.1109/MCS.2007.338280.
[3] Guzzella L., Sciarretta A., *Vehicle Propulsion Systems*, Springer (2013).
[4] Chan C.C., *The State of the Art of Electric and Hybrid Vehicles*, Proceedings of the IEEE, vol. 95, no. 4, pp. 704–718 (2007), DOI: 10.1109/JPROC.2007.892489.
[5] Ehsani M., Gao Y., Emadi A., *Modern Electric, Hybrid Electric, and Fuel Cell Vehicles*, CRC Press (2017), DOI: 10.1201/9781420054002.
[6] Han S., Zhang F., Xi J., *A Real Time Energy Management Strategy Based on Energy Prediction for Parallel Hybrid Electric Vehicles*, IEEE Access, vol. 6, pp. 70313–70323 (2018), DOI: 10.1109/ACCESS.2018.2880751.
[7] Musardo C., Rizzoni G., Staccia B., *AECMS: An Adaptive Algorithm for Hybrid Electric Vehicle Energy Management*, Proceedings of the 44th IEEE Conference on Decision and Control, Seville, Spain, pp. 1816–1823 (2005), DOI: 10.1109/CDC.2005.1582424.
[8] Pisu P., Rizzoni G., *A Comparative Study of Supervisory Control Strategies for Hybrid Electric Vehicles*, IEEE Transactions on Control Systems Technology, vol. 15, no. 3, pp. 506–518 (2007), DOI: 10.1109/TCST.2007.894649.
[9] Vikram Mittal, Rajesh Shah, *Energy Management Strategies for Hybrid Electric Vehicles: A Technology Roadmap*, World Electr. Veh. J., vol. 15, no. 9, 424 (2024) DOI: 10.3390/wevj15090424.
[10] Yonggang Liu, Yitao Wu, Xiangyu Wang, Liang Li, Yuanjian Zhang, Zheng Chen, *Energy management for hybrid electric vehicles based on imitation reinforcement learning*, Energy, vol. 263, Part C (2023), DOI: 10.1016/j.energy.2022.125890.
[11] Zhou S., Chen Z., Huang D., Lin T., *Model Prediction and Rule Based Energy Management Strategy for a Plugin Hybrid Electric Vehicle with Hybrid Energy Storage System*, IEEE Transactions on Power Electronics, vol. 36, no. 5, pp. 5926–5940 (2021), DOI: 10.1109/TPEL.2020.3028154.
[12] Hu Q., Amini M.R., Wang H., Kolmanovsky I., Sun J., *Integrated Power and Thermal Management of Connected HEVs via Multi Horizon MPC*, 2020 American Control Conference Denver, CO, USA, pp. 3053–3058 (2020), DOI: 10.23919/ACC45564.2020.9147487.
[13] Chen B., Pan X., Evangelou S.A., *Optimal Energy Management of Series Hybrid Electric Vehicles with Engine Start–Stop System*, IEEE Transactions on Control Systems Technology, vol. 31, no. 2, pp. 660–675 (2023), DOI: 10.1109/TCST.2022.3192920.
[14] Accurso F., Zanelli A., Rolando L., Millo F., *Real Time Energy Management Control Strategies for an Electrically Supercharged Gasoline Hybrid Vehicle*, WCX SAE World Congress Experience (2020), DOI: 10.4271/2020011009.
[15] Jungen M., Goerke D., Langwiesner M., Schmiedler S. *et al*., *Analytical Methodology to Derive a Rule Based Energy Management System Enabling Fuel Optimal Operation for a Series Hybrid*, SAE Powertrains, Fuels & Lubricants Meeting, Krakow, Poland (2020), DOI: 10.4271/2020-01-2257.

Early Access

This paper has been accepted for publication in the AEE journal. This is the version, which has not been fully edited and content may change prior to final publication.
Citation information: DOI 10.24425/aee.2027.8065

[16] Anselma P.G., Kollmeyer P., Belingardi G., Emadi A., Multi target *Evaluation of Hybrid Electric Vehicle Powertrain Architectures Considering Fuel Economy and Battery Lifetime*, SAE Technical Paper, 2020370015 (2020), DOI: 10.4271/2020-37-0015.
[17] Ritzmann Johannes, Christon Andreas, Salazar Mauro, Onder Christopher, *Fuel-Optimal Power Split and Gear Selection Strategies for a Hybrid Electric Vehicle*, 14th International Conference on Engines & Vehicles, Capri, Italy (2019), DOI: 10.4271/2019-24-0205.
[18] Biswas A., Rane O., Rathore A., Anselma P. *et al*., *Energy Management System for Input Split Hybrid Electric Vehicle (SiEVT) with Dynamic Coordinated Control and Mode Transition Loss*, WCX SAE World Congress Experience, Detroit & Online, Michigan, United States (2022), DOI: 10.4271/2022-01-0674.
[19] Liu J., Peng H., *Modeling and Control of a Power Split Hybrid Vehicle*, IEEE Transactions on Control Systems Technology, vol. 16, no. 6, pp. 1242–1251 (2008), DOI: 10.1109/TCST.2008.919447.
[20] Bo Zhang, Jiangyan Zhang, Fuguo Xu, Tielong Shen, *Optimal Control of Power Split Hybrid Electric Powertrains with Minimization of Energy Consumption*, Applied Energy, vol. 266 (2020), DOI: 10.1016/j.apenergy.2020.114873.
[21] Zou Y., Huang R., Wu X. *et al*., *Modeling and energy management strategy research of a powersplit hybrid electric vehicle*, Advances in Mechanical Engineering, vol. 12 no. 10 (2020), DOI: 10.1177/1687814020962624.
[22] Zheng Chen, Hongji Gu, Shiquan Shen, Jiangwei Shen, *Energy management strategy for powersplit plugin hybrid electric vehicle based on MPC and double Q learning*, Energy, vol. 245 (2022), DOI: 10.1016/j.energy.2022.123182.
[23] Yang Xueping, Jiang Chaoyu, Zhou Ming, Hu Hengjie, *Bilevel energy management strategy for power split plugin hybrid electric vehicles: A reinforcement learning approach for prediction and control*, Frontiers in Energy Research, vol. 11 (2023), DOI: 10.3389/fenrg.2023.1153390.
[24] Khadhraoui A., Selmi T., Cherif A., *Energy Management of a Hybrid Electric Vehicle*, Engineering, Technology & Applied Science Research, vol. 12, no. 4, pp. 8916–8921 (2022), DOI: 10.48084/etasr.5058.
[25] Unni Keerthi, Sushil Thale, *Energy Consumption Analysis for the Prediction of Battery Residual Energy in Electric Vehicles*, Engineering, Technology & Applied Science Research, vol. 13, no. 3, pp. 11011–11019 (2023), DOI: 10.48084/etasr.5868.
[26] Reddy S.V. Pratap Simha, Vijaya Kumar M., *A New Hybrid Energy Storage System for Electric Vehicle Drive System*, Engineering, Technology & Applied Science Research, vol. 14 no. 6, 1885561(2024), DOI: 10.48084/etasr.9010.
[27] Biswas A., Emadi A., *Energy Management Systems for Electrified Power trains: State of the Art Review and Future Trends*, IEEE Transactions on Vehicular Technology, vol. 68, no. 7, pp. 6453−6467 (2019), DOI: 10.1109/TVT.2019.2914457.
[28] Wang S., Zhang S., Shi D., Sun X., Yang T., *Research on hybrid modeling and predictive energy management for power split hybrid electric vehicle*, Bulletin of the Polish Academy of Sciences Technical Sciences, vol. 69, no. 3, e137064 (2021), DOI: 10.24425/bpasts.2021.137064.
[29] Paplicki P., Wardach M., Bonisławski M., Pałka R., *Simulation and experimental results of hybrid electric machine with a novel flux control strategy*, Archives of Electrical Engineering, vol. 64, no. 1, pp. 37–51 (2015), DOI: 10.1515/aee-2015-0005.
[30] Bena L., Tailor R., Medved D., Mazur D., *Electric vehicle charging management system in the industrial zone*, Archives of Electrical Engineering, vol. 73, no. 2, pp. 433–450 (2024), DOI: 10.24425/aee.2024.149925.

Early Access